

# On the current of a free mode in an elongated basin

F. CRISCIANI

*Former Research Executive, CNR-ISMAR, Trieste, Italy*

(Received: 9 November 2023; accepted: 31 January 2024; published online: 5 April 2024)

**ABSTRACT** The current of a free mode included in a zonally elongated basin is zonal almost everywhere, with the exception of the westernmost and easternmost areas of the fluid domain. The main difference between different circulation fields basically concerns the latitudinal localisation of the maximum and minimum flow. This aspect is investigated by determining how total vorticity selects above localisations. The result is that the latter only depends on the value taken by the total vorticity at the points where the stream function is zero. A set of examples illustrates the results.

**Key words:** intensified current, free mode, zonal flow.

## 1. Introduction

A free mode can be conceived as a seawater body circulating in a finite portion of a beta plane, in the absence of forcing and dissipation. This highly idealised system, representing an ocean area, is governed by the conservation of total vorticity, i.e. relative plus planetary, and an equation in closed-form is easily achieved in the framework of the quasi-geostrophic dynamics. The critical point of the model is that total vorticity depends, in a widely arbitrary way, on the stream function and, due to this fact, the uniqueness of the solution is lost. In the seminal paper of Fofonoff (1954), often cited in textbooks (Krauss, 1973; Hendershott, 1987; Pedlosky, 1987, 1996; Vallis, 2006), this dependence is taken linearly to overcome mathematical intricacies inherent to non-linearity. The notable Fofonoff solution shows the formation of an intensified current close to one, or both, zonal boundaries. This special solution raises the question of verifying if, and how, intensification occurs in the non-linear case without resorting to a definite dependence of the total vorticity on the stream function. In a recent paper, Crisciani and Mosetti (2023) investigated the localisation in latitude of the intensified mass transport in a free and stable mode included in elongated basins. The localisation of the eastward mass transport is univocally determined by the sign of the inverse of the total vorticity at the central latitude of the fluid domain, regardless of the total vorticity. In this investigation, the same model and the same question are reconsidered, but by exploring the latitudinal localisation of the maximum and minimum current, sufficiently far from the meridional boundaries where it is zonal, rather than by exploring the transport as in Crisciani and Mosetti (2023). The maximum current is always eastwards and occurs, in any case, at the northern or southern boundary. The boundary singled out depends only on the total vorticity value in the points where the stream function vanishes. The minimum current is always westward and can assume three configurations, depending, as described above, on the total vorticity value in the points where the stream function vanishes. In two cases, the minimum is localised at the boundary opposite to the maximum and the profile is

monotonic (i.e. only increasing or decreasing). In the remaining, the minimum is in the domain interior and its formation is determined by the presence of a bifurcation of the current field. The conclusion is that the qualitative shape of a zonal current, flowing in a free mode, is largely independent of the details of total vorticity.

## 2. General form of the 2D model solution

The model under investigation is described in full detail in Crisciani and Mosetti (2023). Hypotheses, governing equations, and other aspects are listed below. All the quantities are dimensionless. The rectangular fluid domain  $D$  is included in a specific  $\beta$ - plane:

$$D = \{(x, y) : -\lambda \leq x \leq \lambda, 0 \leq y \leq 1\}. \quad (1)$$

In Eq. 1,  $\lambda \gg 1$  so  $D$  represents a zonally elongated domain. The governing equation of the fluid is conservation, in the steady regime, of its total vorticity at the geostrophic level of approximation, i.e.  $(\delta/L)^2 \nabla^2 \psi + y = Q(\psi)$ . The equation takes the well-known form:

$$(\delta/L)^2 \nabla^2 \psi + y = Q(\psi) \quad (2)$$

where  $Q$  is a differentiable function of its argument. The stream function is assumed to be differentiable up to the third order to assure continuity even to the vorticity gradient. In Eq. 2:

$$(\delta/L)^2 \ll 1 \quad (3)$$

and

$$Q_\psi > 0. \quad (4)$$

Inequality in Eq. 3 assumes that the inertial boundary layer width,  $\delta_i = (U/\beta_0)^{1/2}$ , where  $\beta_0$  is the dimensional planetary vorticity gradient, is significantly smaller than the horizontal length scale,  $L$ , thus allowing a longitudinal boundary-layer treatment of the model solution. Inequality in Eq. 4 guarantees the stability (Blumen, 1968) and uniqueness of the full solution. Models in which  $Q_\psi < 0$  (e.g. Moro, 1987; Pedlosky, 2016) are open to instability and are not amenable to the analysis treated here. Impermeability of boundary  $\partial D$  of Eq. 1 is imposed setting:

$$\psi = 0 \quad \forall (x, y) \in \partial D. \quad (5)$$

From Eqs. 1 to 5, and within the boundary-layer approximation applied in  $x = \pm\lambda$ , the model solution is found in the composite form (Crisciani and Mosetti, 2023):

$$\psi(x, y) = \phi(y) \left\{ 1 - \exp \left[ -\sqrt{Q_\phi} L(x + \lambda) / \delta_l \right] \right\} \left\{ 1 - \exp \left[ \sqrt{Q_\phi} L(x - \lambda) / \delta_l \right] \right\}. \quad (6)$$

In Crisciani and Masetti (2023), the authors have also proved that  $\psi(x, y) = \psi(-x, y)$  and  $\psi(x, \frac{1}{2} - y) \neq \psi(x, \frac{1}{2} + y)$ , regardless of  $Q(\psi)$ . The latter asymmetry provides the mathematical explanation of northward or southward intensification of the flow and is an effect of the planetary vorticity gradient. The latitudinal profile of the zonal current appears to be the most evident feature that characterises solutions for different forms of  $Q(\psi)$  and the next section provides some properties of the profile, which are inferred exclusively from  $Q(0)$ , that is from the value taken by  $Q$  wherever  $\psi$  vanishes, regardless of  $Q(\psi)$ .

### 3. Maximum flow latitude

Owing to the elongated shape of the fluid domain (Eq. 1) and to the smallness of  $(\delta/L)^2$ , the solution in Eq. 6 shows that sufficiently far from the meridional boundaries the dependence of  $\psi(x, y)$  on  $x$  is evanescent. This involves a significant computational simplification and justifies, *a posteriori*, the introduction of an elongated domain. Hence, according to Eq. 6,  $\psi(x, y) = \phi(y)$  and the original governing Eqs. 2 to 5, referred to  $\phi$ , change into the following ordinary, generally non-linear<sup>1</sup> problem:

$$\left( \delta_l / L \right)^2 \phi_{yy} + \phi = Q(\phi) \quad (7)$$

$$\phi(0) = \phi(1) = 0 \quad (8)$$

$$Q_\phi > 0 \quad (9)$$

$$\left( \delta_l / L \right)^2 \ll 1 \quad (10)$$

in the unknown  $\phi$ , where the zonal current:

$$u = -\phi_y. \quad (11)$$

Eqs. 8 and 11 should preliminarily be noted to imply mass conservation  $\int_0^1 u dy = 0$  whence:

$$u_{\min} < 0 < u_{\max} \quad (12)$$

and, therefore,  $u_{\min} \hat{y}$  is westwards and  $u_{\max} \hat{y}$  is eastwards. In this section, the zonal current (Eq. 11) is proven to have no maximum in  $]0, 1[$  and, therefore, the maximum occurs in  $y = 0$  or in  $y = 1$ , or in both of them, according to the following criterion:

<sup>1</sup> Non-linearity of Eq. 1 lies in that of  $Q(\psi)$  so, if  $Q(\psi)$  is linear, Eqs. 1 to 4 are linear as well.

- if  $1/2 - Q(0) > 0$ , then,  $u_{max} = u(1)$ ,
- if  $1/2 - Q(0) < 0$ , then,  $u_{max} = u(0)$ , and
- if  $1/2 - Q(0) = 0$ , then,  $u_{max} = u(0) = u(1)$ .

As previously mentioned,  $Q(0)$  is the value of  $Q$  wherever  $\phi$  vanishes.

As proof by contradiction, assuming that  $u(y)$  has a maximum in  $]0, 1[$ , say  $u_{max} = u(\bar{y})$ , then, both conditions below:

$$u_y(\bar{y})=0 \text{ and } u_{yy}(\bar{y}) < 0 \tag{13}$$

are satisfied. At this point a useful link between  $u_{yy}$  and  $u$ , coming from differentiation of Eq. 7 with the aid of Eq. 11, can be invoked. In fact, with  $(\delta_i/L)^2 \phi_{yyy} + 1 = Q_\phi \phi_y$ , the following can be expressed:

$$u_{yy} = (L/\delta_i)^2 (1 + Q_\phi u). \tag{14}$$

Owing to Eq. 14, the second of the conditions in Eq. 13 implies that  $1 + Q_\phi u(\bar{y}) < 0$ , and recalling Eq. 9, the following is encountered:

$$u_{max} = u(\bar{y}) < -1/Q_\phi < 0 \tag{15}$$

that is:

$$u_{max} < 0. \tag{16}$$

Inequality in Eq. 16 contradicts Eq. 12, so the second relationship of Eq. 13 must be rejected. In conclusion, no maximum of  $u(y)$  occurs in  $]0, 1[$ . The second part of the proof starts from the integration of Eq. 7 on  $0 \leq y \leq 1$  by using position in Eq. 11, that is:

$$(\delta_i/L)^2 [u(0) - u(1)] + 1/2 = \int_0^1 Q(\phi) dy. \tag{17}$$

Integration by parts of the right side of Eq. 17 gives:

$$\begin{aligned} \int_0^1 Q(\phi) dy &= [yQ(\phi)]_{y=0}^{y=1} - \int_0^1 yQ_\phi \phi_y dy = Q[\phi(1)] - \int_{\phi(0)}^{\phi(1)} yQ_\phi d\phi = \\ &= Q(0) - \int_0^0 yQ_\phi d\phi = Q(0). \end{aligned} \tag{18}$$

Substitution of Eq. 18 into Eq. 17 yields, after a trivial rearrangement:

$$u(1) - u(0) = (L/\delta_i)^2 [1/2 - Q(0)]. \tag{19}$$

Eq. 19 shows that:

$$\begin{aligned}
 1/2 - Q(0) > 0 &\Rightarrow u(1) = u(0) + (L/\delta_i)^2 [1/2 - Q(0)] \\
 1/2 - Q(0) < 0 &\Rightarrow u(0) = u(1) + (L/\delta_i)^2 [Q(0) - 1/2]. \\
 1/2 = Q(0) &\Rightarrow u(0) = u(1)
 \end{aligned} \tag{20}$$

Due to the amplifying effect of  $(L/\delta_i)^2$  caused by Eq. 10, Eqs. 20 lead to the following conclusions:

$$\begin{aligned}
 1/2 - Q(0) > 0 &\Rightarrow u_{\max} = u(1) \\
 1/2 - Q(0) < 0 &\Rightarrow u_{\max} = u(0) \\
 1/2 = Q(0) &\Rightarrow u_{\max} = u(0) = u(1)
 \end{aligned} \tag{21}$$

that complete the proof. Thus, once  $Q(\phi)$  is given, the maximum current latitude is easily established, *a priori*, according to the sign of  $1/2 - Q(0)$ . From a physical point of view, Eqs. 21 are a consequence of the lack of frictional retardation of the flow, in particular at the boundaries where free slippage can occur.

Remark: the averaging on  $0 \leq y \leq 1$  of relative vorticity at the geostrophic level of approximation, that is  $\langle \zeta_0 \rangle = \int_0^1 \phi_{yy} dy$ , shows that:

$$\langle \zeta_0 \rangle = u(0) - u(1). \tag{22}$$

Hence, Eqs. 21 and 22 correlate  $u_{\max}$  and  $\langle \zeta_0 \rangle$  as follows:

$$\begin{aligned}
 u_{\max} = u(1) &\Leftrightarrow \langle \zeta_0 \rangle < 0 \\
 u_{\max} = u(0) &\Leftrightarrow \langle \zeta_0 \rangle > 0 \\
 u_{\max} = u(0) = u(1) &\Leftrightarrow \langle \zeta_0 \rangle = 0.
 \end{aligned}$$

Although  $\langle \zeta_0 \rangle$  is an integral feature of the current field, from the above correlation the eastward current is argued to be sharply peaked along the wall where it takes its maximum value, in accordance with the phenomenology of current intensification.

#### 4. Minimum flow latitude

In dealing with the minimum flow latitude, intervals  $Q(0) < 0$ ,  $Q(0) > 1$  and  $0 \leq Q(0) \leq 1$  are taken into consideration separately. The equation:

$$u_y = (L/\delta_l)^2 [y - Q(\phi)], \quad (23)$$

which is nothing but an equivalent version of Eq. 7, will be useful.

$Q(0) < 0$  is assumed. This inequality implies, *a fortiori*,  $Q(0) < 1/2$  and hence, owing to Eq. 21:

$$u_{\max} = u(1). \quad (24)$$

In section 4, it has already been proven that no maximum occurs in  $]0, 1[$ .

Moreover, by applying Eq. 23, the following is found:

$$u_y(0) = -(L/\delta_l)^2 Q(0) > 0. \quad (25)$$

No minimum is proven to occur in  $]0, 1[$ .

As proof by contradiction  $u(y)$  is assumed to have a minimum in  $]0, 1[$ , say  $u_{\min} = u(y')$ . Then, in an interval to the left of  $y'$ ,  $u_y < 0$ , whereas, in an interval to the right of  $y = 0$ ,  $u_y > 0$ , according to Eq. 25. This means that a maximum of  $u$  occurs somewhere in interval  $]0, y'[ \subset ]0, 1[$ , in contradiction with what has been proven in section 3. Thus, the assumption that  $u(y)$  has a minimum in  $]0, 1[$  must be rejected and, therefore, Eq. 24 recalled:

$$u_{\min} = u(0). \quad (26)$$

In other words, inequality  $Q(0) < 0$  implies that  $u(y)$  is a monotonic increasing function in the full  $[0, 1]$  interval.

At this point,  $Q(0) > 1$  is assumed. This inequality implies, *a fortiori*,  $Q(0) > 1/2$  and, hence, owing to Eq. 21:

$$u_{\max} = u(0). \quad (27)$$

By using Eq. 23 in the form:

$$u_y(1) = (L/\delta_l)^2 [1 - Q(0)] < 0$$

and in full analogy with the previous proof, we can demonstrate that inequality  $Q(0) > 1$  implies that  $u(y)$  is a monotonic decreasing function in the full  $[0, 1]$  interval and:

$$u_{\min} = u(1). \quad (28)$$

Ultimately,  $0 \leq Q(0) \leq 1$  is assumed. In this case the minimum can occur in  $]0, 1[$ . In this section, a sufficient condition is obtained for the minimum, under the hypothesis of a certain

limitation on  $Q(0)$ . More precisely, we prove that if:

$$0 \leq Q(0) \leq 1 \quad (29)$$

and<sup>2</sup>

$$\lim_{y \rightarrow 0^+} Q^{-1}(y) < \infty, \quad \lim_{y \rightarrow 1^-} Q^{-1}(y) < \infty \quad (30)$$

then

$$u_{\min} = u(\tilde{y}) \quad (31)$$

for some  $\tilde{y} \in ]0, 1[$ . The proof relies on the assumption of the validity of the boundary-layer approximation of the actual solution. We necessarily resort to this method as it does not demand hypotheses on  $Q(\phi)$  outside of Eqs. 29 and 30 and, for this reason, it is expected to hold for a wide class of model solutions.

Proof: the following is obtained from Eq. 23:

$$u_y(0) = -(L/\delta_l)^2 Q(\phi(0)) = -(L/\delta_l)^2 Q(0) < 0 \quad (32)$$

$$u_y(1) = (L/\delta_l)^2 [1 - Q(\phi(1))] = (L/\delta_l)^2 [1 - Q(0)] > 0. \quad (33)$$

Due to Eqs. 32 and 33:

$$u_y(y'') = 0 \quad (34)$$

for some  $y' \in ]0, 1[$ . To verify that  $u_{yy}(y') > 0$ , the auxiliary function is preliminarily introduced:

$$\phi^{\text{int}} = Q^{-1}(y), \quad (35)$$

which approximates  $\phi$  in the domain interior where all quantities,  $\phi_{yy}$ ,  $y$ ,  $Q(\phi)$ , have the same order of magnitude<sup>3</sup>. Due to the smallness of  $(\delta_l/L)^2$ , the dominant balance is only between  $y$  and  $Q(\phi)$ , whence Eq. 35 follows. Attention should be drawn to the fact that  $u^{\text{int}} = -\phi_y^{\text{int}} = -Q_y^{-1} < 0$ , in accordance with Greenspan (1962). Thus, Eqs. 30 are equivalent to stating that  $\phi^{\text{int}}(0)$  and  $\phi^{\text{int}}(1)$  are finite. The double inequality in Eq. 29 separately implies that  $Q^{-1}(0) \leq 0$  and  $0 \leq Q^{-1}(1)$ , that is to say:

<sup>2</sup>  $Q^{-1}(y)$  is the inverse function of  $Q(\phi)$ , not its reciprocal in the algebraic sense.

<sup>3</sup> Although  $\phi^{\text{int}}$  is a local approximation of  $\phi$ , it is not a solution as it cannot satisfy boundary conditions in Eq. 8 because  $Q^{-1}(y)$  is a monotonic increasing function of its argument.

$$\phi^{int}(0) \leq 0, \phi^{int}(1) \geq 0. \tag{36}$$

At this point, the standard boundary-layer method can be applied to both  $[0, 1[$  and  $]0, 1]$  intervals. In the first case:

$$\phi = \phi^{int}(y) + \chi(\eta) \tag{37}$$

where  $\eta = Ly/\delta_l$  is the boundary-layer coordinate and  $\chi(\eta)$  is the related ‘correction’ term. The resulting solution, expressed by means of the sole original variable, is:

$$\phi(y) = \phi^{int}(y) - \phi^{int}(0) \exp\left\{-\left[Q_\phi(\phi^{int}(0))\right]^{1/2} Ly / \delta_l\right\}. \tag{38}$$

Quite analogously, in the second case the following is encountered:

$$\phi(y) = \phi^{int}(y) - \phi^{int}(1) \exp\left\{\left[Q_\phi(\phi^{int}(1))\right]^{1/2} L(y-1) / \delta_l\right\}. \tag{39}$$

With the aid of the shorthand notations:

$$A_0 = \left[Q_\phi(\phi^{int}(0))\right]^{1/2}, \quad A_1 = \left[Q_\phi(\phi^{int}(1))\right]^{1/2}$$

the overall solution, deriving from Eqs. 38 and 39, can be expressed as:

$$\phi(y) = \phi^{int}(y) - \phi^{int}(0) \exp\left[-A_0 Ly / \delta_l\right] - \phi^{int}(1) \exp\left[A_1 L(y-1) / \delta_l\right]. \tag{40}$$

From Eq. 40, the following is obtained:

$$u_{yy} = -\phi_{yyy} = -\phi_{yyy}^{int} + (L/\delta_l)^3 \left\{-\phi^{int}(0) A_0^3 \exp\left[-A_0 Ly / \delta_l\right] + \phi^{int}(1) A_1^3 \exp\left[-A_0 L(y-1) / \delta_l\right]\right\} \tag{41}$$

Due to the amplifying factor,  $(L/\delta_l)^3$ , that multiplies the second term to the right of Eq. 41, the sign of  $u_{yy}$  is the same as that of the quantity in curly brackets. Owing to Eq. 36, the latter is positive, and therefore:

$$u_{yy} > 0 \quad \forall y. \tag{42}$$

Ultimately, from Eqs. 34 and 42,  $y'' = \tilde{y}$  is concluded to be a minimum of the zonal velocity. This completes the proof.



In the weaker hypothesis:

$$0 < Q(0) < 1 \quad (43)$$

in place of Eq. 29, at a certain latitude,  $\hat{y} \in ]0, 1[$ , a flow bifurcation occurs and is such that two independent circulating systems are generated in the fluid domain: one cyclonic in  $D_1 = \{(x, y) : -\lambda \leq x \leq \lambda, \hat{y} < y \leq 1\}$  and the other anti-cyclonic in  $D_2 = \{(x, y) : -\lambda \leq x \leq \lambda, 0 < y < \hat{y}\}$ . The global effect is a westward current in the basin interior, the minimum of which has just been highlighted by Eqs. 34 and 42. The proof resorts to the partial boundary layer solutions in Eqs. 38 and 39, as follows.

Initially, a right interval of  $y = 0$  is considered where, according to Eq. 38:

$$\phi(y) = \phi^{\text{int}}(y) - \phi^{\text{int}}(0) \exp[-A_0 L y / \delta_l]. \quad (44)$$

From Eq. 44, the following can be expressed:

$$\phi(0) = 0 \quad (45)$$

and

$$\phi_y(0) = \phi_y^{\text{int}}(0) + (L / \delta_l) A_0 \phi^{\text{int}}(0). \quad (46)$$

Due to the amplifying factor,  $L / \delta_l$ , that multiplies the second term to the right of Eq. 46, the sign of  $\phi_y(0)$  is the same as the sign of  $\phi^{\text{int}}(0)$ , whence:

$$\phi_y(0) < 0 \quad (47)$$

follows. In turn, Eqs. 45 and 47 imply that:

$$\phi(y) < 0 \quad (48)$$

in a suitable right interval of  $y = 0$ . Analogously, starting from Eq. 39, the following can be expressed:

$$\phi(1) = 0 \quad (49)$$

and

$$\phi_y(1) < 0. \quad (50)$$

In turn, Eqs. 49 and 50 imply that:

$$\phi(y) > 0 \tag{51}$$

in a suitable left interval of  $y = 1$ . Ultimately, from Eqs. 48 and 51 the existence of a point  $\hat{y} \in ]0,1[$  is such that  $\phi(\hat{y}) = 0$  is immediately proved. Given that  $\phi(\hat{y}) = 0$  means  $\psi(x, \hat{y}) = 0$ , the bifurcation appears to be quite evident.

### 5. Summary

The results of sections 3 and 4 are summarised below, with reference to the distribution of the  $Q$ -variability range:

- |  |   |
|--|---|
| 1) $Q(0) < 0 \Rightarrow u_{max} = u(1),$          | $u_{min} = u(0),$ $u$ increases monotonically,            |
| 2) $0 \leq Q(0) < 1/2 \Rightarrow u_{max} = u(1),$ | $u_{min} = u(\hat{y}),$ for some $\hat{y} \in ]0,1[,$     |
| 3) $Q(0) = 1/2 \Rightarrow u_{max} = u(1) = u(0),$ | $u_{min} = u(\tilde{y}),$ for some $\tilde{y} \in ]0,1[,$ |
| 4) $1/2 < Q(0) \leq 1 \Rightarrow u_{max} = u(0),$ | $u_{min} = u(\hat{y}),$ for some $\hat{y} \in ]0,1[,$     |
| 5) $Q(0) > 1 \Rightarrow u_{max} = u(0),$          | $u_{min} = u(1),$ $u$ decreases monotonically.            |

If  $0 < Q(0) < 1$  a flow bifurcation occurs at latitude  $\hat{y} \in ]0,1[$ .

Explicit examples in the next section will elucidate the above results.

### 6. Examples

The solution of the problem in Eqs 7 to 10 is unique (if any) and can be singled out (at least in principle) once the  $(\delta_1/L)^2$  value is fixed and the form of function  $Q(\phi)$  is given.

Recalling that:

$$(\delta_1 / L)^2 = U / \beta_0 L^2 \tag{52}$$

the choice of velocity scale  $U$  and length scale  $L$  must satisfy the following requests:

$$O(U / f_0 L) < 1 \tag{53}$$

in order for the Rossby number  $\varepsilon = \frac{U}{f_0 L}$  to be consistent with the geostrophic nature of Eq. 7 and:

$$O(\beta_0 L / f_0) < 1 \tag{54}$$

for the validity of the  $\beta$ - plane approximation. Inspired by the actual values observed in the real ocean, the following is taken into consideration (reference is intended to SI units):

$$U = 2 \times 10^{-2}, \quad L = 5 \times 10^5. \tag{55}$$

From Eqs. 52 and 55,  $(\delta/L)^2 = 8 \times 10^{-3}$  is obtained and, consequently,  $L/\delta_1 \approx 11.2$ . Moreover,  $U/f_0 L = 4 \times 10^{-4}$  and  $\beta_0 L/f_0 = 5 \times 10^{-2}$  are obtained and, therefore, inequalities in Eqs. 53 and 54 are verified as well.

The choice of  $Q(\phi)$  is subject to condition in Eq. 9. For the rest, outside the linear case, there is no particular indication in the literature to this regard. Much less, suggestions of physical nature are lacking. The following is assumed:

$$Q(\phi) = \tan^{-1}(\phi) + C \tag{56}$$

where  $C$  is a constant. With  $O(C) \leq 1$ ,  $O(Q) = 1$ ,  $Q$  balances the left side of Eq. 7. It should be noted that  $Q_\phi = 1 / (1 + \phi^2) > 0$  and, therefore, all solutions are stable. Given that  $Q(0) = C$ , the constant  $C$  is set from time to time in a way compatible with one of the five cases listed in section 5. The meridional profiles of the zonal current are commented below.

In Fig. 1, case 1 is considered for  $C = -1/2$  and the resulting monotonic increasing function  $u(y)$  is depicted. The dimensionless current is included between extremes  $u = -5.4$  and  $u = 15.8$ . Correspondingly, the dimensional (starred)  $u^* = 2 \times 10^{-2} u$  runs from  $-0.11$  to  $0.32 \text{ ms}^{-1}$ . The 2D solution is a single-gyre model in which the return (eastward) current is entirely confined within interval  $0.7 < y \leq 1$ , as shown in Fig. 1.

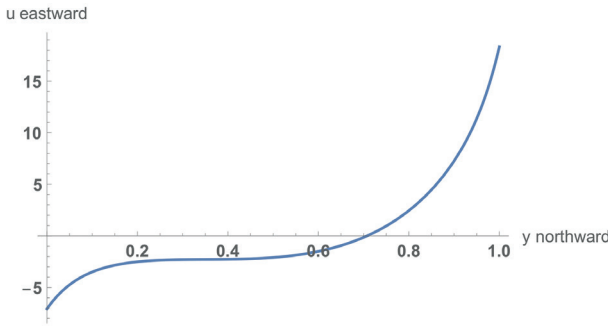


Fig. 1 - Solution for  $Q(\phi)$  given by Eq. 47 with  $C = -1/2$ .

In Figs. 2, 3, and 4, cases 2, 3, and 4 are considered for  $C = 1/4$ ,  $C = 1/2$ , and  $C = 3/4$ , respectively. As long as  $0 < C < 1$ , in all these cases the 2D circulation bifurcates into two separate gyres: one anti-cyclonic, to the north of a certain latitude, and another cyclonic, to the south of it. This configuration determines, on the whole, the observed westward current, at a certain distance from both the zonal boundaries, which is compensated by two return flows close to the boundaries, as shown in Figs. 2, 3, and 4. The maximum eastward current varies from  $u \approx 4.5$  to  $u \approx 8$  and, correspondingly, the dimensional (starred) velocity,  $u^* = 2 \times 10^{-2} u$ , runs from  $9 \times 10^{-2} \text{ ms}^{-1}$  to  $1.6 \times 10^{-1} \text{ ms}^{-1}$ . The minimum westward current does not exceed  $u = -1$ , that is  $u^* = -2 \times 10^{-2} \text{ ms}^{-1}$ . At first glance it would seem that asymmetry  $\psi(x, 1/2-y) \neq \psi(x, 1/2+y)$ , cited in section 2 and proved in Crisciani and Mosetti (2023), is not consistent with Fig. 3 where the zonal current is openly symmetric around  $y = 1/2$ . Indeed, the above asymmetry can be extended as follows. If, besides  $\psi(x, 0) = \psi(x, 1) = 0$ ,  $\psi(x, \hat{y}) = 0$  is also considered for a certain  $0 < \hat{y} < 1$  interval, then, then the following can be proven:

$$\psi(x, \hat{y}/2 - y) \neq \psi(x, \hat{y}/2 + y) \quad 0 \leq y \leq \hat{y} \tag{57}$$

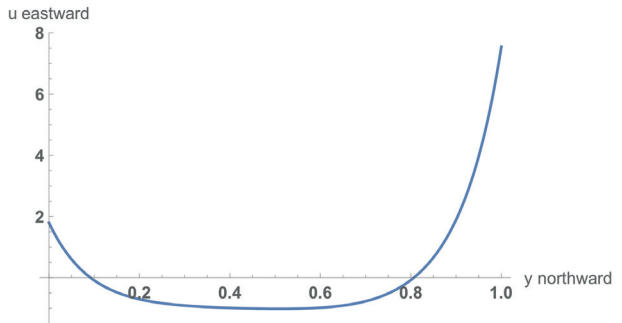


Fig. 2 - Solution for  $Q(\phi)$  given by Eq. 47 with  $C = 1/4$ .

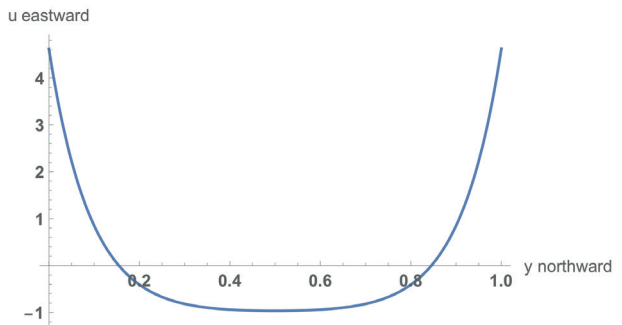


Fig. 3 - Solution for  $Q(\phi)$  given by Eq. 47 with  $C = 1/2$ .

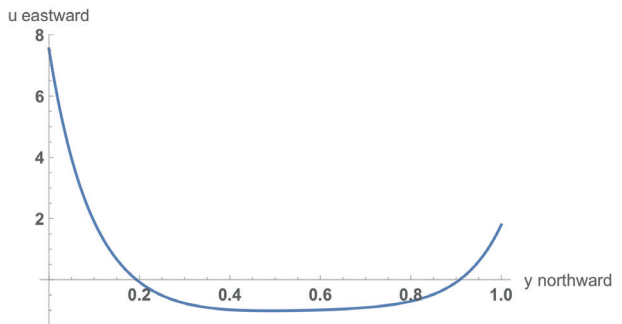


Fig. 4 - Solution for  $Q(\phi)$  given by Eq. 47 with  $C = 3/4$ .

and

$$\psi(x, (\hat{y}+1)/2-y) \neq \psi(x, (\hat{y}+1)/2+y) \quad \hat{y} \leq y \leq 1. \tag{58}$$

In the case of Fig. 3,  $\hat{y} = 1/2$  so Eq. 57 applies to  $\phi(y)$  in  $0 \leq y \leq 1/2$  and Eq. 58 applies in  $1/2 \leq y \leq 1$ . For explanatory purposes, further details of case 4 are reported in Fig. 5.

Fig. 5a is a plot of  $\phi(y)$  for  $C = 3/4$  (case 4) in which the zero of  $\phi$  in  $\hat{y} \approx 0.77$  is the latitude of the flow bifurcation.

Fig. 5b shows the streamlines of the solution for  $C = 3/4$  (case 4) in which the double-gyre system and the intensification near the southern boundary are evident. Unfortunately, the visual resolution at the meridional boundaries is rather poor.

Fig. 5c compensates for the last aspect of Fig. 5b and provides a zoom of the streamlines in

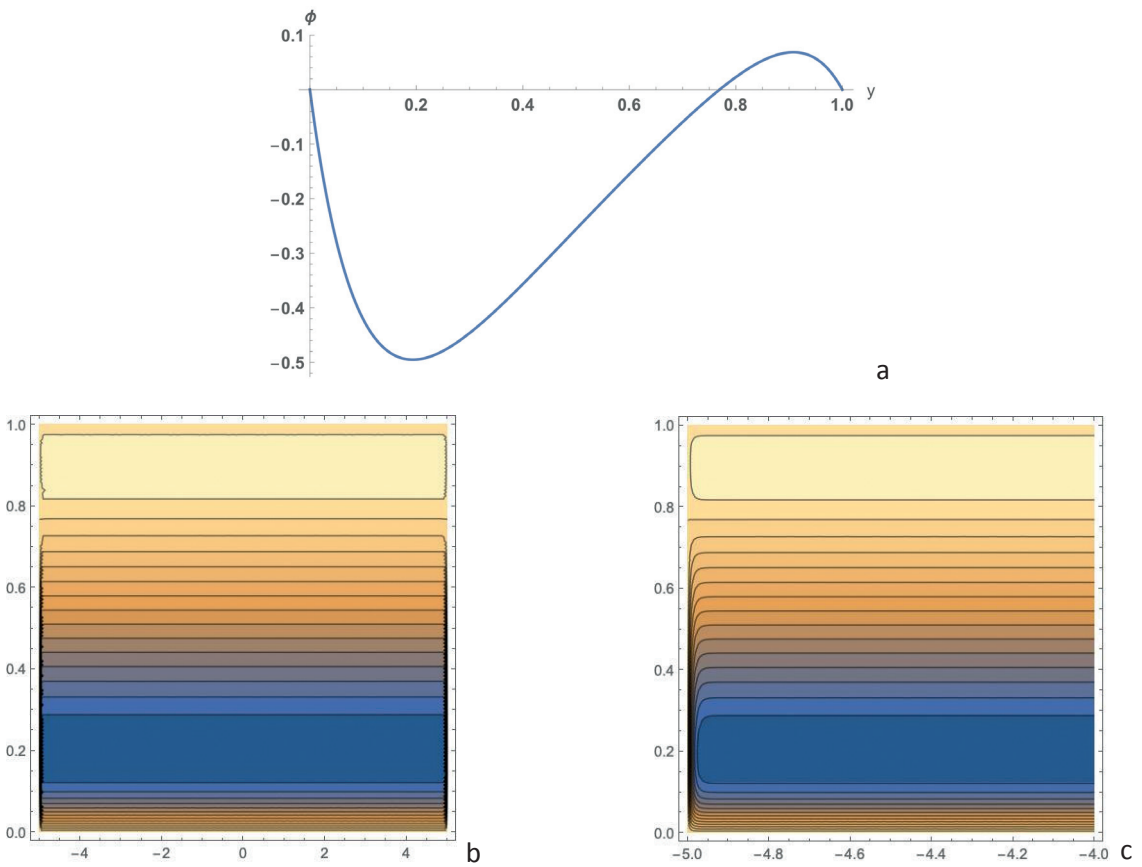


Fig. 5 - Plot of  $\phi(y)$ . This shows the change of sign in  $\hat{y} \approx 0.77$ , which indicates the presence of a pair of counter-rotating gyres in the 2D solution (a). Streamlines of the full solution (b). Zoom of the full solution shown in panel b in the proximity of the western boundary (c).

the restricted interval of  $-5 \leq y \leq -4$ . In this figure the bending of the streamlines, in proximity of the western boundary, is clearly highlighted.

In Fig. 6, case 5 is considered for  $C = 3/2$  and the resulting monotonic decreasing function,  $u(y)$ , is depicted. The dimensionless current is included between extremes  $u = -5.4$  and  $u = 15.8$ . Correspondingly, the dimensional (starred)  $u^* = 2 \times 10^{-2} u$  runs from  $-0.11$  to  $0.32 \text{ ms}^{-1}$ . The 2D solution is a single-gyre model in which the return (eastward) current is entirely confined within interval  $0 \leq y < 0.3$ , as shown in Fig. 6.

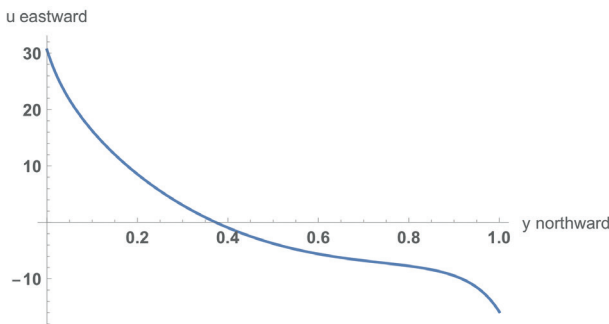


Fig. 6 - Solution for  $Q(\phi)$  given by Eq. 47 with  $C = -3/2$ .

## 7. Concluding remarks

Part of this investigation is related to the paper by Crisciani and Mosetti (2023), whose main result deals with the intensification of zonal mass transport  $\mathbf{M}_S = M_S \hat{i}$ ,  $\mathbf{M}_N = M_N \hat{i}$  defined as:

$$M_S = \int_0^Y u dy, \quad M_N = \int_{1-Y}^1 u dy. \quad (59)$$

In Eq. 59,  $Y$  is the cross-transport width of both  $\mathbf{M}_S$  and  $\mathbf{M}_N$ , which is fixed in such a way that points  $(x, Y)$  and  $(x, 1-Y)$  belong to sub-domain  $D^{int}$  where  $\phi = \phi^{int}$ . Crisciani and Mosetti (2023) proved that:

$$\begin{aligned} Q^{-1}(1/2) > 0 &\Rightarrow M_N > 0 \\ Q^{-1}(1/2) < 0 &\Rightarrow M_S > 0 \\ Q^{-1}(1/2) = 0 &\Rightarrow \mathbf{M}_S = \mathbf{M}_N. \end{aligned} \quad (60)$$

According to Eqs. 60, the transport is always eastwards, but in the first case the intensification is northwards, in the second southwards and, in the third, both northwards and southwards. Note that these conclusions cannot be extended to the current in place of the transport by considering  $\lim_{Y \rightarrow 0} \int_0^Y u dy$  and  $\lim_{Y \rightarrow 0} \int_{1-Y}^1 u dy / Y$ . This is due to the fact that the condition that points  $(x, Y)$  and  $(x, 1-Y)$  belong to  $D^{int}$  could be inconsistent with the evaluation of  $\lim_{Y \rightarrow 0}$ . However, given that  $Q^{-1}(1/2) > 0 \Leftrightarrow Q(0) < 1/2$ , we ascertain that the same condition on  $Q$  that implies  $M_N > 0$  (see Eqs. 60) implies also  $u_{max} = u(1)$  according to Eq. 21. The same conclusion can easily be drawn for the remaining cases.

**Acknowledgments.** The author is grateful to Renzo Mosetti for the useful discussions and help in preparing section 6.

## REFERENCES

- Blumen W.; 1968: *On the stability of quasi-geostrophic flow*. J. Atmos. Sci., 25, 929-931.
- Crisciani F. and Mosetti R.; 2023: *Intensified flows in free modes*. Bull. Geoph. Ocean., 64, 331-346.
- Fofonoff N.P.; 1954: *Steady flow in a frictionless homogeneous ocean*. J. Mar. Res., 13, 254-262.
- Greenspan H.P.; 1962: *A criterion for the existence of inertial boundary layers in the oceanic circulation*. Proc. Natl. Acad. Sci. U.S.A., 48, 2034-2039, doi: 10.1073/pnas.48.12.2034.
- Hendershott M.C.; 1987: *Single layer models of the general circulation*. In: Abarbanel H.D.I. and Young W.R. (eds), General circulation of the ocean, Springer-Verlag, Berlin, Germany, 291 pp.
- Krauss W.; 1973: *Dynamics of the homogeneous and quasi homogeneous ocean*. Gebruder Borntraeger, Berlin - Stuttgart, Germany, 302 pp.
- Moro B.; 1987: *On the inertial motion of a homogeneous ocean*. Dyn. Atmos. Oceans, 11, 1-17.
- Pedlosky J.; 1987: *Geophysical fluid dynamics*. Springer-Verlag, Berlin, Germany, 710 pp.
- Pedlosky J.; 1996: *Ocean circulation theory*. Springer-Verlag, Berlin, Germany, 453 pp.
- Pedlosky J.; 2016: *Fofonoff negative modes*. Fluids, 1, 13, 11 pp., doi:10.3390/fluids1020013.
- Vallis G.K.; 2006: *Atmospheric and oceanic fluid dynamics*. Cambridge University Press, Cambridge, UK, 745 pp., doi: 10.1017/CBO9780511790447.

Corresponding author: Fulvio Crisciani  
E-mail: fulviocrisciani@gmail.com